

NeXSP heavy ion results on elliptic flow at RHIC and connection with thermalization

R. Andrade¹, F. G. Bassi¹, Y. Hamam¹, T. Kodama², O. Socolowski Jr.³, and B. Tavares²

¹ Instituto de Física, USP,
C.P. 66318, 05315-970 São Paulo-SP, Brazil

² Instituto de Física, UFRJ,
C.P. 68528, 21945-970 Rio de Janeiro-RJ, Brazil

³ CTA/ITA,
Praça Marechal Duardo Gómes 50, CEP 12228-900 São José dos Campos-SP,
Brazil

Received 1 January 2004

Abstract. Elliptic flow at RHIC is computed event-by-event with NeXSP heavy ion. Reasonable agreement with experimental results on $v_2(\eta)$ is obtained. Various effects are studied as well: reconstruction of impact parameter direction, freeze out temperature, equation of state (with or without crossover), emission mechanism.

Keywords: Elliptic flow, relativistic nuclear collisions, thermalization

PACS: 24.10.Nz, 25.75.Ld, 25.75.-q

1. Motivation

Hydrodynamics seems a correct tool to describe RHIC collisions however $v_2(\eta)$ is not well reproduced as shown by Hirano et al. [1]. These authors suggested that this might be due to lack of thermalization. Heinz and Kolb [2] presented a model with partial thermalization and obtained a reasonable agreement with data. The question addressed in this work is whether lack of thermalization is the only explanation for this disagreement between data and theory for $v_2(\eta)$.

2. Brief description of NeX SP heR IO

The tool we use is the hydrodynamical code called NeX SP heR IO. It is a junction of two codes.

The SP heR IO code is used to compute the hydrodynamical evolution. It is based on Smoothed Particle Hydrodynamics, a method originally developed in astrophysics and adapted to relativistic heavy ion collisions [3]. Its main advantage is that any geometry in the initial conditions can be incorporated.

The NeXus code is used to compute the initial conditions T , j and u on a proper time hypersurface [4]. An example of initial condition for one event is shown in figure 1.

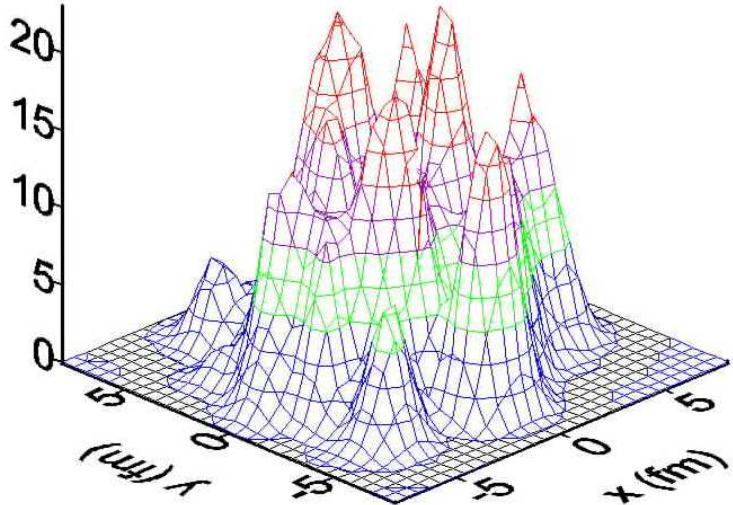


Fig. 1. Example of initial energy density in the $x = 0$ plane.

NeX SP heR IO is run many times, corresponding to many different events or initial conditions. In the end, an average over final results is performed. This mimics experimental conditions. This is different from the canonical approach in hydrodynamics where initial conditions are adjusted to reproduce some selected data and are very smooth.

This code has been used to study a range of problems concerning relativistic nuclear collisions: effect of fluctuating initial conditions on particle distributions [5], energy dependence of the kaon effective temperature [6], interferometry at RHIC [7], transverse mass distributions at SPS for strange and non-strange particles [8].

3. Results

3.1. Theoretical vs. experimental computation

Theoretically, the impact parameter angle b is known and varies in the range of the centrality window chosen. The elliptic flow can be computed easily through

$$\langle v_2^b(\phi) \rangle = \langle \frac{\int_0^R d^2N = d \cdot d \cdot \cos[2(\phi - b)] d}{\int_0^R d^2N = d \cdot d} \rangle \quad (1)$$

The average is performed over all events in the centrality bin. This is shown by the lowest solid curve in figure 2.

Experimentally, the impact parameter angle β is reconstructed and a correction is applied to the elliptic flow computed with respect to this angle, to correct for the reaction plane resolution. For example in a Hobobs-like way [9]

$$\langle v_2^{b;rec}(\phi) \rangle = \langle \frac{v_2^{obs}(\phi)}{\langle \cos[2(\beta - \phi)] \rangle} \rangle \quad (2)$$

where

$$v_2^{obs}(\phi) = \frac{\int_0^P d^2N = d \cdot d \cdot \cos[2(\beta - \phi)]}{\int_0^P d^2N = d \cdot d} \quad (3)$$

and

$$\beta = \frac{1}{2} \tan^{-1} \frac{\int_0^P d \cdot \sin 2 \phi}{\int_0^P d \cdot \cos 2 \phi} \quad (4)$$

In the hit-based method, $\beta \leq 0$ and $\beta \geq 0$ are determined for subevents $\phi < 0$ and $\phi > 0$ respectively and if v_2 is computed for a positive (negative) β , the sum in v_2 , equation 3, is over particles with $\phi < 0$ ($\phi > 0$).

In the track-based method, $\beta \leq 0$ and $\beta \geq 0$ are determined for subevents $2.05 < j < 3.2$ and v_2 is obtained for particles around $0 < \phi < 1.8$ and reflected (there is also an additional $\pi/2$ in the reaction plane correction in equation 2).

In figure 2, we also show the results for $v_2^{obs}(\phi)$ for both the hit-based (dashed line) and track-based (dotted line) methods. We see that both curves lie above the theoretical $\langle v_2^b(\phi) \rangle$ (solid) curve. So dividing them by a cosine to get $\langle v_2^{b;rec}(\phi) \rangle$ will make the disagreement worse: $\langle v_2^b(\phi) \rangle$ and $\langle v_2^{b;rec}(\phi) \rangle$ are different.

Since the standard way to include the correction for the reaction plane resolution (equation 2) seems inapplicable, we need to understand why. When we look at the distribution $d^2N = d \cdot d$ obtained with NeXSP heRIO, it is not symmetric with respect to the reaction plane. This happens because the number of produced particles is finite. Therefore we must write

$$\frac{d^2N}{d \cdot d} = v_0^b(\phi) [1 + \sum_{n=1}^X 2v_n^b(\phi) \cos(n(\phi - b)) + \sum_{n=1}^X 2v_n^{0b}(\phi) \sin(n(\phi - b))] \quad (5)$$

$$= v_0^{obs}(\phi) [1 + \sum_{n=1}^X 2v_n^{obs}(\phi) \cos(n(\phi - \beta)) + \sum_{n=1}^X 2v_n^{0obs}(\phi) \sin(n(\phi - \beta))] \quad (6)$$

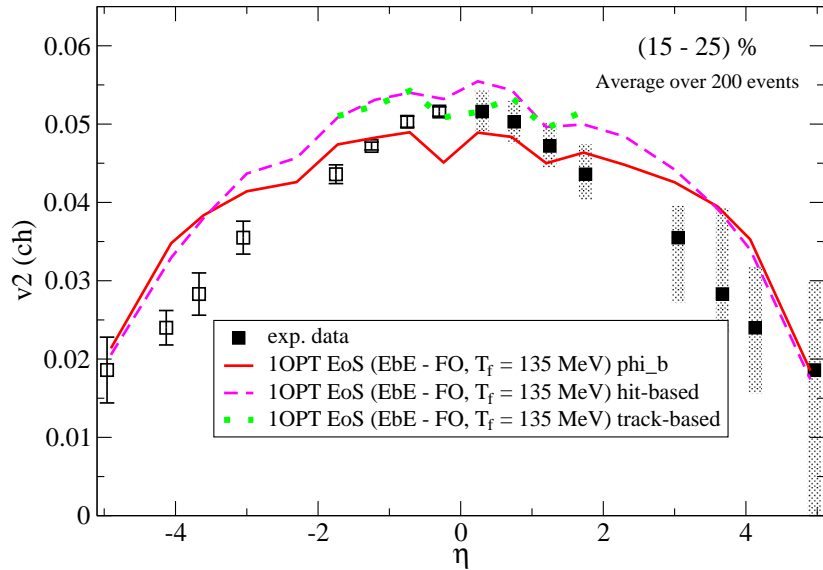


Fig. 2. Comparison of various ways of computing v_2 : solid line is using the known impact parameter angle ϕ_b , dashed and dotted lines is using the reconstructed impact parameter angle ϕ_2 . Data are from PHOBOS [9]. For more details see text.

It follows that

$$v_2^{\text{obs}}(\eta) = v_2^b(\eta) \cos(2(\phi_2 - \phi_b)) + v_2^b(\eta) \sin(2(\phi_2 - \phi_b)) \quad (7)$$

We see that due to the term in sine, we can indeed have $\langle v_2^{\text{obs}}(\eta) \rangle$ larger than $\langle v_2^b(\eta) \rangle$, as in figure 2. (The sine term does not vanish upon averaging on events because if a choice such as equation 4 is done for ϕ_2 , $v_2^b(\eta)$ and $\sin(2(\phi_2 - \phi_b))$ have same sign.) In the standard approach, it is supposed that $d^2N = d\eta d\phi$ is symmetric with respect to the reaction plane and there are no sine terms in the Fourier decomposition of $d^2N = d\eta d\phi$ (equation 5); as a consequence, $v_2^{\text{obs}}(\eta) = v_2^b(\eta)$.

Since the experimental results for elliptic flow are obtained assuming that $d^2N = d\eta d\phi$ is symmetric around the reaction plane, we cannot expect perfect agreement of our $\langle v_2^b(\eta) \rangle$ with them. In the following we use the theoretical method, i.e. $\langle v_2^b(\eta) \rangle$, to make further comparisons.

3.2. Study of various effects which can influence the shape of $v_2(\eta)$

In all comparisons, the same set of initial conditions is used, scaled to reproduce $dN/d\eta$ for $T_{\text{freeze-out}} = 135$ MeV.

First we study the effect of the freeze out temperature on the pseudo-rapidity and transverse momentum distributions as well as $v_2(\eta)$ (this last quantity is shown

in figure 3). We found that $v_2(\eta)$ and $d^2N/dp_t dp_\eta$ favor $T_{f,out} = 135$ MeV, so this temperature is used thereafter.

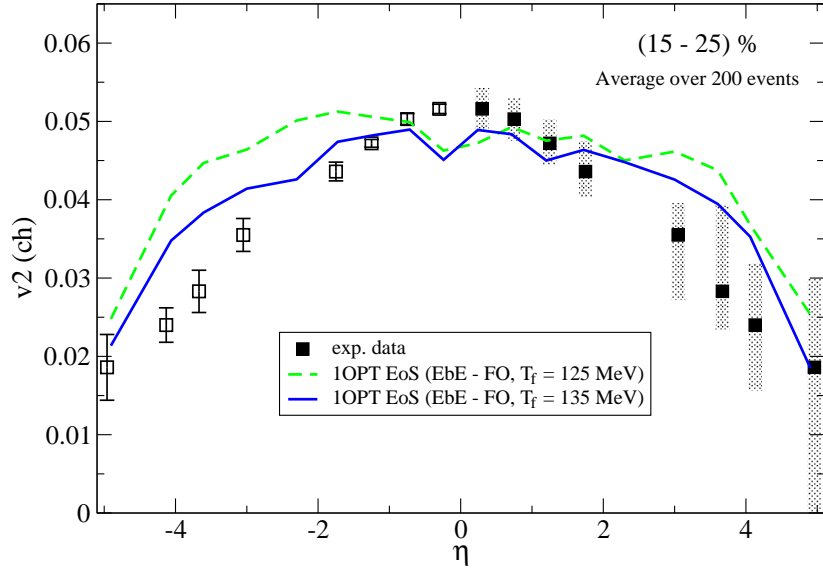


Fig. 3. Comparison of $v_2(\eta)$ for two freeze out temperatures.

We now compare results obtained for a quark matter equation of state with first order transition to hadronic matter and with a crossover (for details see [10]). We have checked that the η and p_t distributions are not much affected. We expect larger v_2 for cross over because there is always acceleration and this is indeed what is seen in figure 4.

We then compare results obtained for freeze out and continuous emission [11]. Again, we have checked that the η and p_t distributions are not much affected. We expect earlier emission, with less flow, at large $|\eta|$ regions, therefore, narrower $v_2(\eta)$ and this is indeed what is seen in figure 5.

Finally, we note that compared to Hirano's pioneering work with smooth initial conditions, the fact that we used event-by-event initial conditions seems crucial: we immediately avoid the two bump structure. To check this, it is interesting to study what we would get with smooth initial conditions. We obtained such conditions by averaging the initial conditions of 30 Nexus events. Again, we have checked that the η and p_t distributions are not much affected but preliminary results shown in figure 6 indicate that now v_2 is very different, having a bumpy structure.

4. Summary

$v_2(\eta)$ was computed with NeXSPheR ID at RHIC energy. Event-by-event initial conditions seem important to get the right shape of $v_2(\eta)$ at RHIC. Other features seem less important: freeze out temperature, equation of state (with or without crossover), emission mechanism. Finally, we have shown that the reconstruction of the impact parameter direction η_2 , as given by eq. (4), gives $v_2^{\text{obs}}(\eta) > v_2^b(\eta)$, when taking into account the fact that the azimuthal particle distribution is not symmetric with respect to the reaction plane.

Lack of thermalization is not necessary to reproduce $v_2(\eta)$. The fact that there is thermalization outside mid-pseudorapidity is reasonable given that the (averaged) initial energy density is high there (figure not shown). A somewhat similar conclusion was obtained by Hirano at this conference, using color glass condensate initial conditions for a hydrodynamical code and emission through a cascade code [12].

We acknowledge financial support by FAPESP (2004/10619-9, 2004/13309-0, 2004/15560-2, CAPES/PROBRAL, CNPq, FAPERJ and PRONEX).

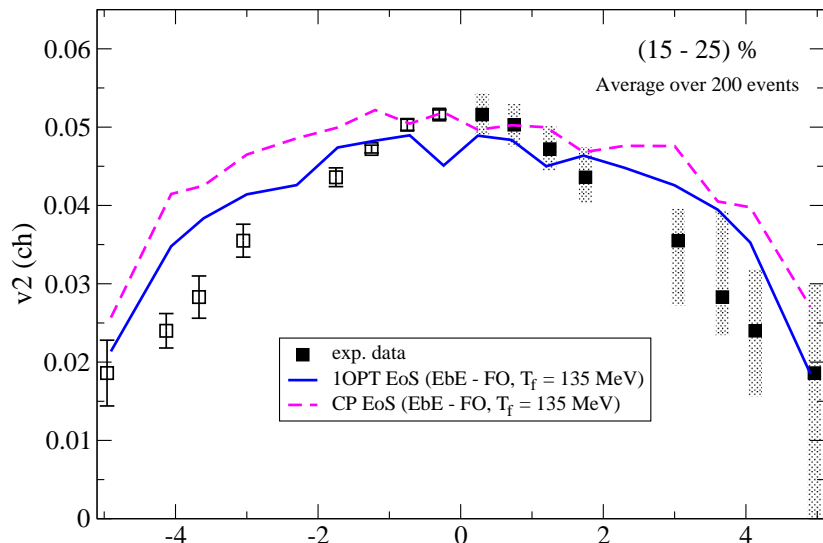


Fig. 4. Comparison of $v_2(\eta)$ for first order transition and critical point equations of state.

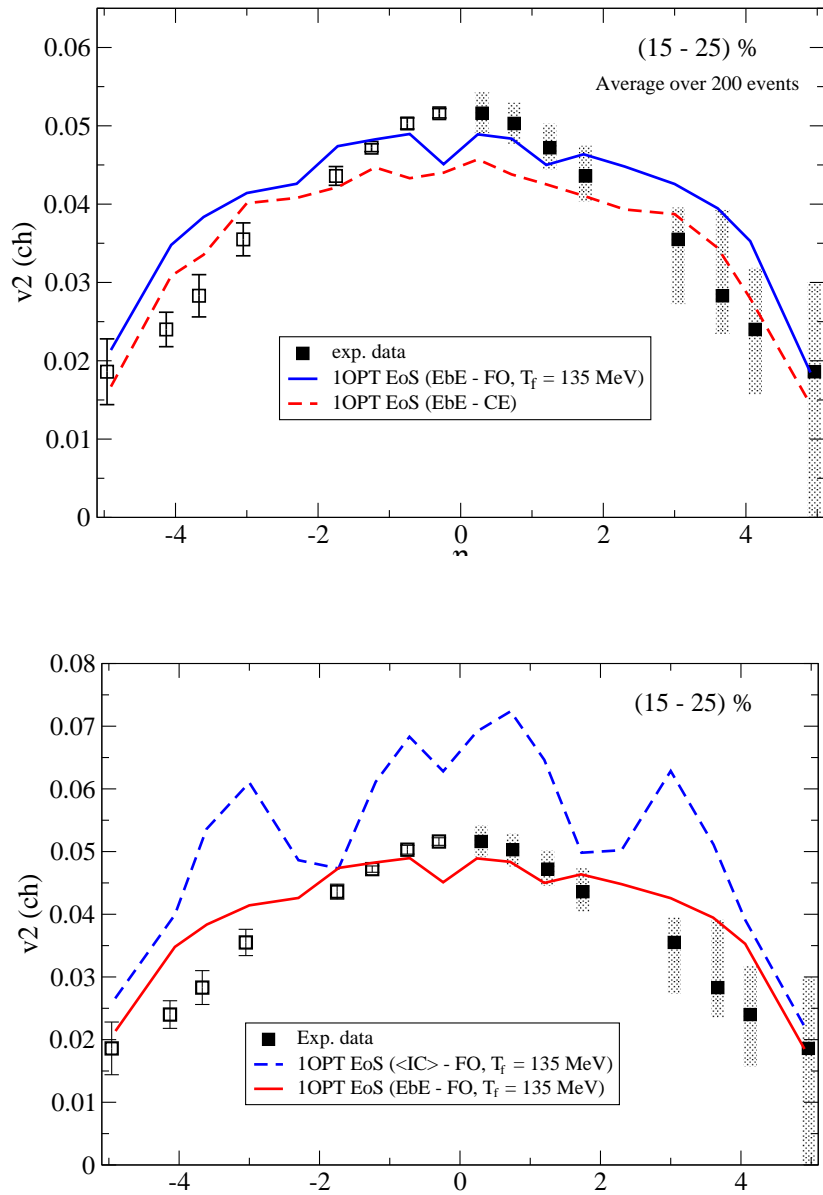


Fig. 6. Comparison of $v_2(\eta)$ computed event-by-event and with smooth initial conditions.

5. References

References

1. T. Hirano, *Phys. Rev. C* 65 (2001) 011901. T. Hirano and K. Tsuchida, *Phys. Rev. C* 66 (2002) 054905.
2. U. Heinz and P. F. Kolb, *J. Phys. G* 30 (2004) S1229.
3. C. E. Aguiar, T. Kodama, T. Ochiai and Y. Hamaguchi, *J. Phys. G* 27 (2001) 75.
4. H. J. Drescher, F. M. Lu, S. O. Stapchenko, T. Pierog and K. Wemer, *Phys. Rev. C* 65 (2002) 054902. Y. Hamaguchi, T. Kodama and O. Socolowski Jr., *Braz. J. Phys.* 35 (2005) 24.
5. C. E. Aguiar, Y. Hamaguchi, T. Kodama and T. Ochiai, *Nucl. Phys. A* 698 (2002) 639c.
6. M. G. Azdzicki, M. I. Gorenstein, F. Grassi, Y. Hamaguchi, T. Kodama and O. Socolowski Jr., *Braz. J. Phys.* 34 (2004) 322; *Acta Phys. Pol. B* 35 (2004) 179.
7. O. Socolowski Jr., F. Grassi, Y. Hamaguchi and T. Kodama, *Phys. Rev. Lett.* 93 (2004) 182301.
8. F. Grassi, Y. Hamaguchi, T. Kodama and O. Socolowski Jr., *J. Phys. G* 30 (2005) S1041.
9. B. B. Back, M. D. Baker, D. S. Barton et al., *Phys. Rev. Lett.* 89 (2002) 222301. B. B. Back, M. D. Baker, M. Ballintijn et al., *nucl-ex/0407012*.
10. Y. Hamaguchi, R. Andrade, F. Grassi et al., *hep-ph/0510096; hep-ph/0510101*.
11. F. Grassi, Y. Hamaguchi and T. Kodama, *Phys. Lett. B* 355 (1995) 9; *Z. Phys. C* 73 (1996) 153.
12. T. Hirano, *nucl-th/0510005*.